Gradient Independent Translation via Differential Morphology

C. Andrew Segall and Scott T. Acton
Oklahoma Imaging Laboratory
School of Electrical and Computer Engineering
Oklahoma State University
Stillwater, OK 74078

Abstract

A new multi-scale image enhancement mechanism is presented. Derived from the differential representation of the morphological filters, it approximates a median filter and alleviates many of the image blotching and noise preserving characteristics of morphological filtering. In one-dimension, the process is shown to be idempotent and to converge. In two dimensions, experimental results demonstrate convergence and display the ability to remove impulsive noise. Gradient Independent Translation avoids the two dimensional convergence problems of the median filter and does not involve the expensive rank-ordering of pixel intensities. Describing a scale space with median filter characteristics, it provides a multi-scale analysis method suitable for compression, coding, and feature extraction.

1. Introduction

Grayscale morphology is traditionally realized with the nonlinear maximum and minimum operators over windowed sets [4]. However, it has been demonstrated that multi-scale morphological filters can be modeled by differential equations [1,2]. In this differential approach, morphological filters can be viewed as the translation of signal gradients, revealing many salient properties.

The concept of a morphological gradient representation is easily illustrated. Consider the discrete signal sequence shown in Figure 1(a), consisting of a finite impulse of width *W*. Eroding the sequence with a structuring element of width greater than *W*/2 will remove the impulse and is shown in Figures 1(b)-(d). Calculating the signal gradient with simple differences demonstrates the differential

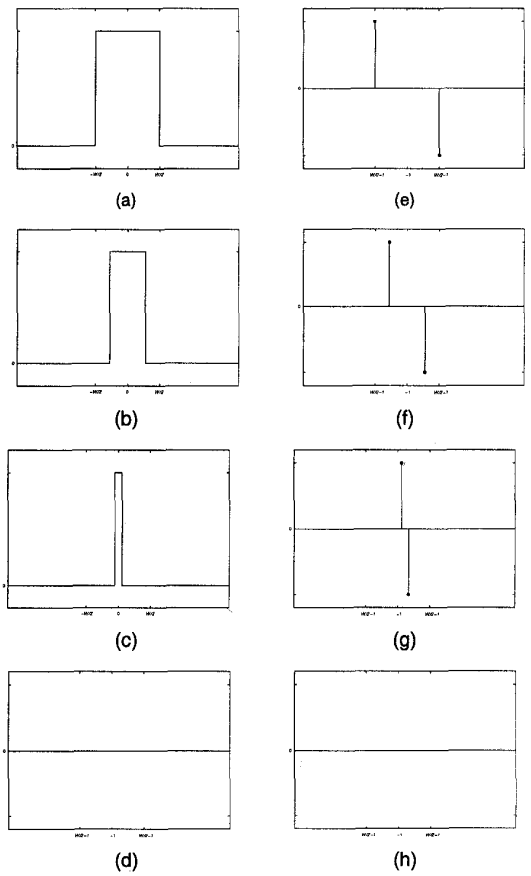

Figure 1 Eroding a step function with structuring elements of different size. From top to bottom: (a) the original step function; (b) the step function eroded with a small structuring element; (c) the structuring element eroded with a larger structuring element; (d) the step function eroded with a structuring element larger than *W*/2. The equivalent differential representations are shown in (e)-(h).

This material is based upon work supported by the U.S. Army Research Office under grant number DAAH04-95-1-0255.

0-8186-8821-1/98 $10.00 © 1998 IEEE

approach. The gradient representation of the initial impulse sequence is shown in Figure 1(e). Gradients of the filtered results are shown in Figure 1(f)-(h). As displayed in the figures, the erosion operator moves positive gradients to the right and negative gradients to the left. The impulse is removed when the gradients collide.

In differential form, erosion may be expressed as

$$\nabla \mathbf{I}_{t+\Delta t}(x) = \nabla^{+}\mathbf{I}_{t}\left(x-\frac{\Delta t}{2}\right)+\nabla^{-}\mathbf{I}_{t}\left(x+\frac{\Delta t}{2}\right), \quad (1)$$

where $t+\Delta t$ is the width of the structuring element, $\nabla \mathbf{I}_1$ is the original image (where $t=1$), ∇^{+} is the maximum value of either the gradient or zero, ∇^{-} is the minimum value of either the gradient or zero, Δt is the time step, and t is the scale parameter. For discrete implementation, Δt would be unity. Dilation reverses the direction of gradient propagation and is expressed as

$$\nabla \mathbf{I}_{t+\Delta t}(x) = \nabla^{+}\mathbf{I}_{t}\left(x+\frac{\Delta t}{2}\right)+\nabla^{-}\mathbf{I}_{t}\left(x-\frac{\Delta t}{2}\right). \quad (2)$$

The sequential combination of these fundamental operators results in an infinite number of ways that a gradient may be translated. The open-close and close-open morphological filter sequences attempt to remove features independent of intensity, but all morphological operations inherently bias region removal by intensity. For example, the open-close filter tends to link neighboring negative-going impulses, while the close-open filter tends to link neighboring positive going impulses. In a gradient representation, this is evident in the spatial bias of each particular gradient path, as gradients are forced to sequentially interact along the prescribed route. Smoothing operations possessing these characteristics are not robust and may introduce severe image distortions, as demonstrated in the results.

One potential solution to the intensity bias of morphological filtering is to initially restrict structuring element size. A signal is filtered with a small structuring element, which is gradually increased until the desired scale is attained [3]. The distance over which two gradients may interact is increased as the structuring element is enlarged. An alternative solution is presented in the next section. The approach completely removes the influence of gradient direction on translation, allowing gradients to move and interact without spatial preference. The resulting smoothing operator approximates a median filter under certain conditions. Convergence and scaling properties make it well suited for multi-scale image analysis applications.

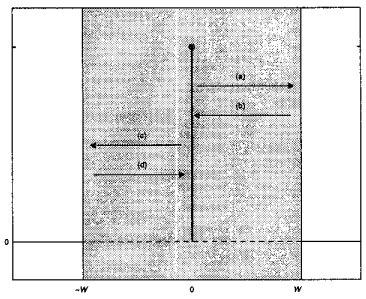

Figure 2 Differential representation of a morphological open-close filter. Positive gradients are moved by (a) erosion, (b) dilation, (c) dilation, and (d) erosion. A negative gradient would follow the opposite path.

2. Gradient Independent Translation

The morphological open-close filter serves as the basis for proposing a spatially unbiased smoothing process. Defined as an erosion-dilation-dilation-erosion sequence, it is described in differential form as

$$\nabla \mathbf{I}_{t+\Delta t}(x) = \begin{cases} \nabla^{+}\mathbf{I}_{t}\left(x-\frac{\Delta t}{2}\right)+\nabla^{-}\mathbf{I}_{t}\left(x+\frac{\Delta t}{2}\right), & 1 < t \le W \\ \nabla^{+}\mathbf{I}_{t}\left(x+\frac{\Delta t}{2}\right)+\nabla^{-}\mathbf{I}_{t}\left(x-\frac{\Delta t}{2}\right), & W < t \le 2W \\ \nabla^{+}\mathbf{I}_{t}\left(x+\frac{\Delta t}{2}\right)+\nabla^{-}\mathbf{I}_{t}\left(x-\frac{\Delta t}{2}\right), & 2W < t \le 3W \\ \nabla^{+}\mathbf{I}_{t}\left(x-\frac{\Delta t}{2}\right)+\nabla^{-}\mathbf{I}_{t}\left(x+\frac{\Delta t}{2}\right), & 3W < t \le 4W \end{cases} \quad (3)$$

where W is equal to the structuring element width and t is the scale parameter. The path of a positive gradient is shown in Figure 2.

With the open-close filter, positive gradients are moved to the right, returned to their initial position, moved to the left, and returned again. The positive gradients traveling along this path intrinsically favor interaction with negative gradients toward the right. Only after encountering all of the negative gradients does the positive gradient travel towards its left. Images filtered with these smoothing operators can possess many undesirable attributes, such as image blotching, streaking, and noise preservation.

Addressing this concern, we propose a new filtering process. Assigning half of the gradient magnitude to travel along the traditional path while the remainder moves in the opposite direction, any positive/negative bias realized by spatial position is removed. The proposed smoothing mechanism is described as

$$\nabla_A \mathbf{I}_1 = \nabla_B \mathbf{I}_1 = \frac{1}{2}\nabla \mathbf{I}_1, \tag{4}$$

where

$$\nabla_A \mathbf{I}_{t+\Delta t}(x) = \begin{cases} \nabla_A^+ \mathbf{I}_t\left(x - \frac{\Delta t}{2}\right) + \nabla_A^- \mathbf{I}_t\left(x + \frac{\Delta t}{2}\right), & 1 < t \le W \\ \nabla_A^+ \mathbf{I}_t\left(x + \frac{\Delta t}{2}\right) + \nabla_A^- \mathbf{I}_t\left(x - \frac{\Delta t}{2}\right), & W < t \le 2W \\ \nabla_A^+ \mathbf{I}_t\left(x + \frac{\Delta t}{2}\right) + \nabla_A^- \mathbf{I}_t\left(x - \frac{\Delta t}{2}\right), & 2W < t \le 3W \\ \nabla_A^+ \mathbf{I}_t\left(x - \frac{\Delta t}{2}\right) + \nabla_A^- \mathbf{I}_t\left(x + \frac{\Delta t}{2}\right), & 3W < t \le 4W \end{cases}, \tag{5}$$

$$\nabla_B \mathbf{I}_{t+\Delta t}(x) = \begin{cases} \nabla_B^+ \mathbf{I}_t\left(x + \frac{\Delta t}{2}\right) + \nabla_B^- \mathbf{I}_t\left(x - \frac{\Delta t}{2}\right), & 1 < t \le W \\ \nabla_B^+ \mathbf{I}_t\left(x - \frac{\Delta t}{2}\right) + \nabla_B^- \mathbf{I}_t\left(x + \frac{\Delta t}{2}\right), & W < t \le 2W \\ \nabla_B^+ \mathbf{I}_t\left(x - \frac{\Delta t}{2}\right) + \nabla_B^- \mathbf{I}_t\left(x + \frac{\Delta t}{2}\right), & 2W < t \le 3W \\ \nabla_B^+ \mathbf{I}_t\left(x + \frac{\Delta t}{2}\right) + \nabla_B^- \mathbf{I}_t\left(x - \frac{\Delta t}{2}\right), & 3W < t \le 4W \end{cases}, \tag{6}$$

and

$$\nabla \mathbf{I}_{t+\Delta t} = \nabla_A \mathbf{I}_{t+\Delta t} + \nabla_B \mathbf{I}_{t+\Delta t}. \tag{7}$$

While Gradient Independent Translation removes the spatial bias of the smoothing interactions, it also guarantees idempotence in one dimension. Reapplication of the filter process will require the gradients to move along the same path as previous filter sequences. Restrained to this path, gradients will interact with one another during the first filter sequence. Those not removed will then return to their original spatial location. Additional filtering sequences will propel the surviving gradients along the same paths, but without further information reduction, as contributing components were previously removed in the first sequence.

3. Analysis

Gradient Independent Translation is equivalent to a weighted average of morphological filters in one dimension. Consider the gradient path described in (5). Positive gradients initially travel to the right and, therefore, only interact with gradients moving in the opposite direction. Two possible gradients could be encountered. If a negative gradient is moving in accordance to (5), it could interact with the positive gradient. As the positive and negative gradients collide, the smaller gradient would be removed and the larger gradient would be reduced. Thus, the magnitudes of the gradients described by (5) would be modified.

A second gradient also has the potential to interact with the positive gradient of (5). Positive gradients moving in accordance to (6) travel in directions opposite to the positive gradients described by (5). When the paths of the positive gradients intersect, the gradients could interact. However, Gradient Independent Translation does not modify gradients that have the same sign. Each gradient will continue in its original direction, and gradient magnitudes will be unchanged. Positive gradients described by (6) do not have a direct effect on positive gradients described by (5).

It can also be shown that these gradients cannot indirectly influence one another. Positive gradients described by (5) only interact with negative gradients moving in accordance with (5). For a gradient described by (6) to affect the positive gradient of (5), the negative gradient of (5) must be modified. From the definition of Gradient Independent Translation, negative gradients described by (6) will not modify the positive gradients of (5), as they both move with the same speed and in the same direction. Thus, the positive gradients of (5) are independent of the gradient movement described by (6).

The separability of the two gradient movement descriptions, (5) and (6), is evident following the analysis of the three other gradient classes. After considering the same conditions presented above for a negative gradient moving according to (5), a positive gradient described by (6) and a negative gradient described by (6), it is seen that the gradient movements of (5) and (6) are independent. This allows Gradient Independent Translation to be expressed as a linear combination of morphological operators. A morphological open-close operation is described in (5), and a morphological close-open operation is described in (6). With these equivalencies, Gradient Independent Translation may be expressed in one dimension as

$$\mathbf{I}_W = \frac{((\mathbf{I}_1 \bullet \mathbf{W}) \circ \mathbf{W}) + ((\mathbf{I}_1 \circ \mathbf{W}) \bullet \mathbf{W})}{2}, \tag{8}$$

where $\mathbf{I}_W$ is the filtered signal at solution time W, $\mathbf{I}_1$ is the original image, $\mathbf{W}$ is a one dimensional structuring element of length W, $((\mathbf{I} \bullet \mathbf{W}) \circ \mathbf{W})$ is the close-open filtering of $\mathbf{I}$ with $\mathbf{W}$, and $((\mathbf{I} \circ \mathbf{W}) \bullet \mathbf{W})$ is the open-close filtering of $\mathbf{I}$ by $\mathbf{W}$.

Representing Gradient Independent Translation as a weighted average of the morphological open-close and close-open filters provides an intuitive description of the new smoothing mechanism. However, the morphological representation does not appear to be valid in higher dimensions. Consider the synthetic image shown in

Figure 3(a). Two objects are present, and Figures 3(b)-(c) depict the initial gradient movement induced by (5) and (6), respectively. In one dimension, positive gradients described by (5) and negative gradients described by (6) travel in the same direction and do not interact. However, gradients moving in higher dimensional spaces traverse more complex paths. Figure 3(d) illustrates locations where gradients moving in accordance to (5) and (6) may interact. With this interaction, the weighted average of the morphological filters no longer describes Gradient Independent Translation.

4. Experimental Results

To illustrate the characteristic smoothing performance of Gradient Independent Translation, the operator was applied to the cameraman image. In these results, we display the robustness of Gradient Independent Translation in the presence of impulsive noise to that of the morphological and median filters.

Numerical simulation of Gradient Independent Translation was accomplished using a two dimensional extension of the one-dimensional operator. Separable approximations were initially employed but displayed excessive spatial bias. Horizontal objects were completely processed before vertical features were considered. In removing the spatial bias, an iterative separable method was utilized. First, the original image was divided into filtered and unfiltered components, where $\mathbf{I}_{Filter} = \alpha \cdot \mathbf{I}$ and $\mathbf{I}_{Unfilter} = (1-\alpha) \cdot \mathbf{I}$. Then, the filtered image was processed along its individual rows and columns. The filtered and unfiltered results were then recombined, and the process iterated. A more formal algorithm is currently under development, but experimental results do illustrate convergence of the new operator in two dimensions.

Five nonlinear operators were initially applied to the original cameraman. The operators included the morphological open-close, close-open, average of the open-close and close-open, and the median filter. Results are presented in Figure 4. Stopping conditions for the median filter were arbitrarily defined to be five iterations, and as can be seen, the operator affected a great deal of smoothing. This excessive blurring was evident in the removal of the internal features of the face. The results of the morphological filters and Gradient Independent Translation were similar. Minor feature preservation differences were seen in the interior of the camera, but comparable image structure was preserved.

The benefits of the new method were observed in the presence of noise. Corrupting the cameraman image with 10% salt and pepper noise, the experiment was repeated. Results are presented in Figure 5. Displaying its non-convergent characteristic, the median filter again required

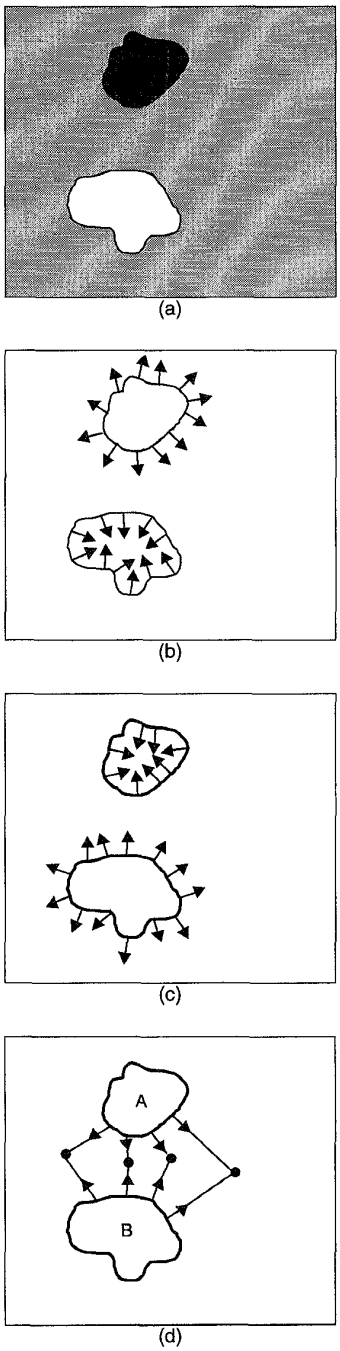

Figure 3 Two dimensional Gradient Independent Translation allows interaction between gradients described by (5) and (6): (a) original image; (b) initial gradient movement according to (5); (c) initial gradient movement according to (6); four locations of potential interaction between negative gradients of (5) and positive gradients of (6).

an arbitrary stopping criterion. While the filter removed the additive noise, it also introduced excessive smoothing. Application of the morphological filters to the noisy imagery exhibited their sensitivity to impulsive noise and their propensity to introduce image blotching. As a result of their intrinsic intensity bias, the morphological filters were unable to remove all outliers. Additionally, image structure was modified. (Notice the alterations to the cameraman's nose, for example.) In contrast, Gradient Independent Translation was capable of removing the noise while preserving image structure.

5. References

[1] L. Dorst and R. van den Boomgaard, "Morphological signal processing and the slope transform," *Signal Processing*, vol.38, pp.79-98, 1994.

[2] P. Maragos, "Differential Morphology and Image Processing," in *IEEE Transactions on Image Processing*, vol.5, pp.922-37, 1996.

[3] A. Morales, T. Acharya, and S. Ko, "Morphological pyramids with alternating sequential filters", in IEEE Transactions on Image Processing, vol.4, no.7, pp.965-977, 1995.

[4] S. Sternberg, "Grayscale Morphology," in Computer, Vision, Graphics, and Image Processing, vol.35, pp.333-355, 1986.

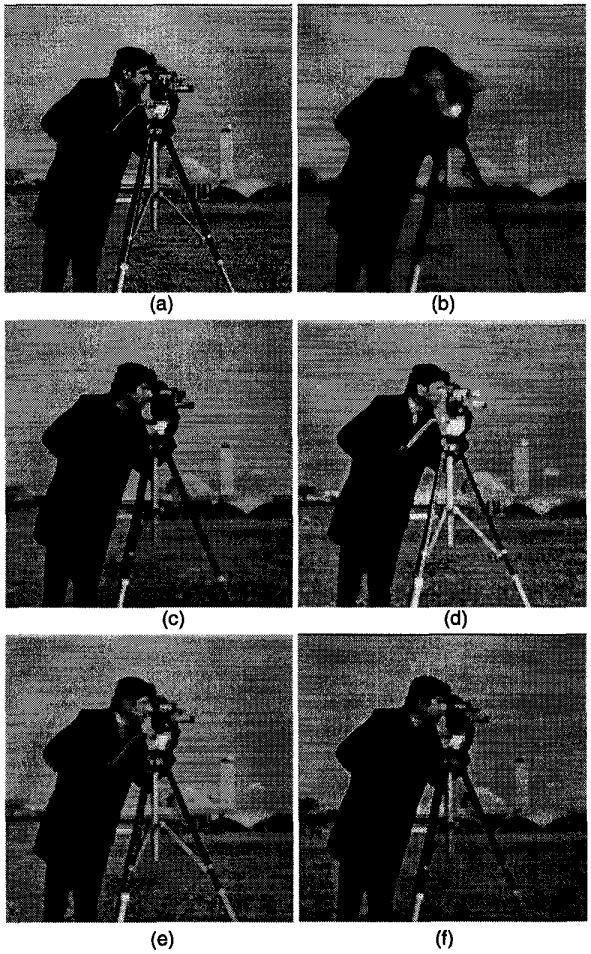

Figure 4 Five nonlinear filters applied to uncorrupted imagery: (a) cameraman image; (b) results obtained using the median filter; (c) results obtained using the morphological open-close operation; (d) results obtained using the morphological close-open; (e) results obtained using the weighted average morphological filter; (f) results obtained using Gradient Independent Translation.

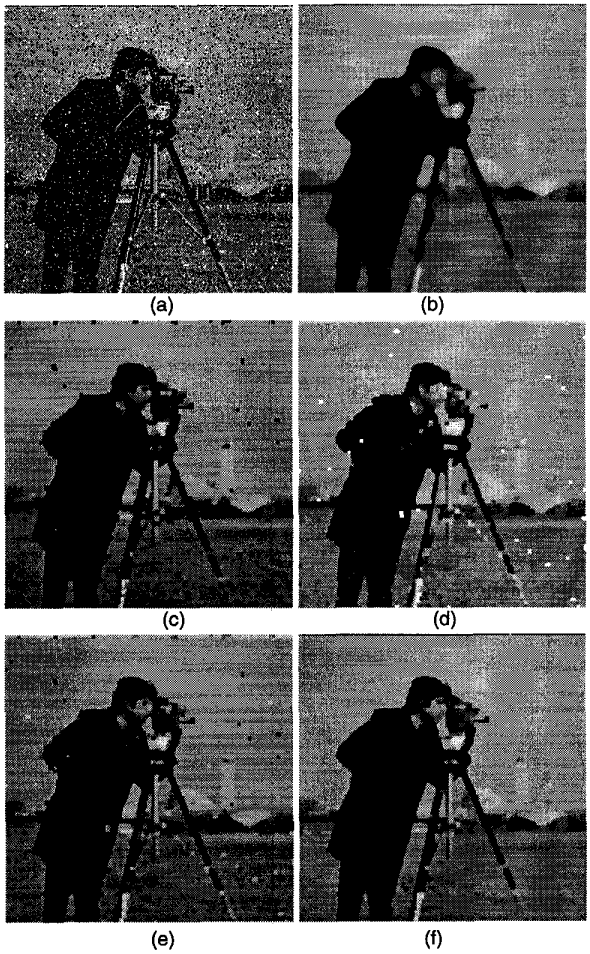

Figure 5 Five nonlinear filters applied to noisy imagery: (a) cameraman image corrupted with 10% salt and pepper noise; (b) results obtained using the median filter; (c) results obtained using the morphological open-close operation; (d) results obtained using the morphological close-open; (e) results obtained using the weighted average morphological filter; (f) results obtained using Gradient Independent Translation.